Supporting Information

Synthesis, microstructures, and gas separation performance of norbornyl bis-benzocyclobutene-Tröger's base polymers derived from pure regioisomers

Xiaofan Hu,[a] Jie Miao,[a] Yuanyuan Pang,[b] Jiayi Zhao,[c] Yao Lu,[a] Heling Guo,[a] Zhen Wang*[a] and Jingling Yan*[a]

[a] Ningbo Institute of Material Technology and Engineering, Chinese Academy of Science, Ningbo 315201, China.

[b] College of Science & Technology, Ningbo University, Cixi 315300, China

[c] Changchun Institute of Applied Chemistry, Chinese Academy of Sciences, Changchun 130022, China.

Email: wz@nimte.ac.cnJingling, jyan@nimte.ac.cn

List of Contents for Supplementary Materials:

EXPERIMENTAL SECTION

Materials

3-Bromo-2-methylaniline, 4-bromo-2,5-dimethylaniline, norbornadiene (NBD), anhydrous 1,4-dioxane, cesium carbonate (Cs_2CO_3), and triphenylphosphine (PPh_3) were purchased from Energy Chemical (Shanghai, China). Dimethoxymethane (DMM) and trifluoroacetic acid (TFA) were obtained from TCI Chemicals (Shanghai, China). All other chemicals were purchased from Titan Scientific Co., Ltd (Shanghai, China).

Monomer Synthesis

All the CANAL-diamines in this work were prepared according to literature procedures, and the pure regioisomers were obtained by column chromatography.[1,2] A representative procedure was shown below.

$Pd(OAc)_2$ (0.045 g, 0.2 mmol), PPh_3 (0.105 g, 0.4 mmol), Cs_2CO_3 (6.52 g, 20 mmol), 3-bromo-2-methylaniline (3.72 g, 20 mmol.), NBD (0.92 g, 10 mmol) 1,4-dioxane(70 mL) were mixed in a 250-mL two-necked flask in a glove box. The flask was then connected to a Schlenk line and heated at 130 °C for 24 hours in argon. Afterwards, the reaction was cooled to a temperature of 60 °C, and the inorganic salts were removed by filtration. The filtrate was concentrated, and *anti*-CANAL-4-$MeNH_2$ and *syn*-CANAL-4-$MeNH_2$ were isolated by column chromatography using a mixture of ethyl acetate and petroleum ether (1:4, *v*:*v*).

***Anti*-CANAL-4-$MeNH_2$** Yield: 42%. Thin layer chromatography (TLC): acetate/petroleum ether = 1/2. R_f = 0.76. ^{1}H NMR (600 MHz, DMSO-d_6): δ 6.53 (d, *J* = 7.6 Hz, 2H), 6.43 (d, *J* = 7.6 Hz, 2H), 4.56 (s, 4H), 3.06 (s, 2H), 3.01 (d, *J* = 3.0 Hz, 2H), 2.17 (s, 2H), 1.88 (s, 6H), 0.63 (s, 2H). ^{13}C NMR (151 MHz, DMSO-d_6): δ 146.34, 145.10, 132.95, 120.05, 116.20, 114.17, 47.54, 47.27, 36.90, 26.39, 12.18. MS (MALDI+): m/z = 302.1791 ($[C_{21}H_{22}N_2]^+$).

***Syn*-CANAL-4-$MeNH_2$** Yield: 24%. TLC: acetate/petroleum ether = 1/2. R_f = 0.65. ^{1}H NMR (600 MHz, DMSO-d_6): δ 6.53 (d, *J* = 7.6 Hz, 2H), 6.43 (d, *J* = 7.6 Hz, 2H), 4.56 (s, 4H), 3.09 (d, *J* = 3.5 Hz, 2H), 2.98 (d, *J* = 3.5 Hz, 2H), 2.25 (s, 1H), 2.09 (s, 1H), 1.90 (s, 6H), 0.64 (s, 2H). ^{13}C NMR (151 MHz, DMSO-d_6): δ 146.32, 145.02, 133.02, 120.02, 116.22, 114.19, 47.64, 47.19, 37.94, 35.87, 26.39, 12.26. MS (MALDI+): m/z = 302.1786 ($[C_{21}H_{22}N_2]^+$).

***Anti*-CANAL-2-Me_2NH_2** Yield: 30%. TLC: acetate/dichloromethane/petroleum ether = 1/4/6. R_f = 0.64. ^{1}H NMR (400 MHz, DMSO-d_6): δ 6.24 (s, 2H), 4.46 (s, 4H), 3.02 (d, *J* = 3.5 Hz, 2H), 2.98 (d, *J* = 3.5 Hz, 2H), 2.19 (s, 2H), 1.99 (s, 6H), 1.86 (s, 6H), 0.64 (s, 2H). ^{13}C NMR (101 MHz, DMSO-d_6): δ 146.51, 144.64, 131.75, 129.25, 114.95, 113.41, 47.07, 46.36, 36.04, 26.57, 16.79, 11.93.

***Syn*-CANAL-2-Me_2NH_2** Yield: 25%. TLC: acetate/dichloromethane/petroleum ether = 1/4/6. R_f = 0.61. ^{1}H NMR (400 MHz, DMSO-d_6): δ 6.24 (s, 2H), 4.46 (s, 4H), 3.03 (d, *J* = 3.4 Hz, 2H), 2.97 (d, *J* = 3.4 Hz, 2H), 2.20 (s, 1H), 2.18 (s, 1H), 1.99 (s, 6H), 1.86 (s, 6H), 0.64 (s, 2H). ^{13}C NMR (101 MHz, DMSO-d_6): δ 146.46, 144.54, 131.86, 129.24, 114.99, 113.45, 47.05, 46.38, 36.40, 35.69, 26.57, 16.77, 11.95.

Polymer Synthesis

The CANAL-TB polymers in this study were synthesized according to a reported method.[3,4] A typical polymerization process is shown below.

***Anti*-CANAL-TB-4.** *Anti*-CANAL-4-$MeNH_2$ (1.0104 g 3.34 mmol) and DMM (1.48 mL, 16.7 mmol) were placed into a 50 mL round-bottomed flask cooled by an ice bath. TFA (15 mL) was then added dropwise. Once the solid completely dissolved, the reaction was warmed up to ambient temperature and stirred for another 60 min. The resulting viscous solution was neutralized with ammonium hydroxide solution (5%). The fibrous polymer was collected, Soxhlet extracted with for 24 h, purified by re-dissolution in chloroform and precipitation into methanol, and dried at 120 °C in vacuum for 20 h to produce anti-CANAL-TB-4 (yield: 82%). ^{1}H NMR (400 MHz, $CDCl_3$): δ 6.41 (s, 2H), 4.58 (s, 2H), 4.26 (s, 2H), 3.92 (s, 2H), 3.14 (s, 4H), 2.67-1.77 (m, 8H), 0.76 (s, 2H); FT-IR

(wavenumber, cm^{-1}): 2925, 2846 (C-H vibration), 1458, 1437, 1412 (aromatic C=C vibration), 1346 (C-H rotation), 1198, 1101 (C-N vibration); M_w = 132.5 kg/mol, PDI = 2.13; $T_d^{5\%}$ = 431 °C; S_{BET} = 826 m^2 g^{-1}, total pore volume = 0.62 cm^3 g^{-1} (at P/P_0 = 0.99); CO_2 uptake = 59.3 cm^3 g^{-1}; ρ = 1.013 g/cm^3, FFV_{sim} = 0.319.

***Syn*-CANAL-TB-4.** Yield: 84%. ^{1}H NMR (400 MHz, $CDCl_3$): δ 6.40 (s, 2H), 4.58 (s, 2H), 4.28 (s, 2H), 3.92 (s, 2H), 3.11 (s, 4H), 2.75-1.85 (m, 8H), 0.75 (s, 2H); FT-IR (wavenumber, cm^{-1}): 2927, 2848 (C-H vibration), 1458, 1437, 1412 (aromatic C=C vibration), 1346 (C-H rotation), 1198, 1101 (C-N vibration); M_w = 117.8 kg/mol, PDI = 1.93; $T_d^{5\%}$ = 423 °C; S_{BET} = 855 m^2 g^{-1}, total pore volume = 0.63 cm^3 g^{-1} (at P/P_0 = 0.99); CO_2 uptake = 59.6 cm^3 g^{-1}; ρ = 1.010 g/cm^3, FFV_{sim} = 0.323.

***Anti*-CANAL-TB-2.** Yield: 87%. ^{1}H NMR (400 MHz, $CDCl_3$) δ 4.42 (s, 2H), 4.30-4.14 (m, 2H), 3.86 (s, 2H), 3.14 (s, 4H), 2.65-2.07 (m, *J* = 33.9 Hz, 8H), 1.92 (s, 6H), 0.80 (s, 2H); FT-IR (wavenumber, cm^{-1}): 2920, 2879, 2843 (C-H vibration), 1437 (aromatic C=C vibration), 1354 (C-H rotation), 1198, 1101 (C-N vibration); M_w = 87.2 kg/mol, PDI = 1.87; $T_d^{5\%}$ = 441 °C; S_{BET} = 846 m^2 g^{-1}, total pore volume = 0.65 cm^3 g^{-1} (at P/P_0 = 0.99); CO_2 uptake = 56.8 cm^3 g^{-1}; ρ = 0.972 g/cm^3, FFV_{sim} = 0.323.

***Syn*-CANAL-TB-2** Yield: 85%. ^{1}H NMR (400 MHz, $CDCl_3$): δ 4.42 (s, 2H), 4.23 (s, 2H), 3.86 (s, 2H), 3.11 (s, 4H), 2.59-2.05 (m, 8H), 1.91 (s, 6H), 0.76 (s, 2H); FT-IR (wavenumber, cm^{-1}): 2922, 2879, 2843 (C-H vibration), 1437 (aromatic C=C vibration), 1354 (C-H rotation), 1200, 1101 (C-N vibration); M_w = 103.6 kg/mol, PDI = 2.04; $T_d^{5\%}$ = 443 °C; S_{BET} = 818 m^2 g^{-1}, total pore volume = 0.62 cm^3 g^{-1} (at P/P_0 = 0.99); CO_2 uptake = 55.6 cm^3 g^{-1}; ρ = 0.978 g/cm^3, FFV_{sim} = 0.318.

Membrane Fabrication

The chloroform solution of CANAL-TB polymers (3wt%) were filtered through a 0.45 μm PTFE syringe filters to remove insoluble impurities, and then cast onto flat glass plates. The solvent was removed by slow evaporation at room temperature for 3 days. The resultant membranes were peeled off from the substrate, dired at 120 °C in vacuum for 24 h, soaked in methanol for 24 h, and then dried at 120 °C in vacuum for another 24 h.

Characterization

A Bruker Autoflex III Smartbeam Mass spectrometer with a laser source of λ = 355 nm were used to collect the high resolution MALDI-TOF-MS spectra. The ^{1}H and ^{13}C NMR spectra were obtained using a Bruker 600 spectrometer. Fourier transform infrared (FTIR) spectra were obtained using a Agilent Cary 660 spectrometer, respectively. Gel permeation chromatography was conducted on a a HLC-8420 instrument (Tosoh Co.), using chloroform as the eluent. Thermal gravimetric analysis was performed on a Q55 TGA system (TA Instruments) in nitrogen at a heating rate of 10 °C min^{-1}. N_2 sorption and CO_2 isotherms were measured on an ASAP 2460 instrument (Micromeritics) at 77 K and 273 K, respectively. Wide-angle X-ray diffraction (WAXD) patterns were obtained using a Ultima IV X-ray diffractometer (Rigaku, Japan) with a scanning rate of 0.5 ° min^{-1}. Inter-chain distances (*d*-spacing values) were calculated according to Bragg's equation. Film density (ρ) was determined by using a density balance (FA2104J, Shanghai) at an accuracy of 0.1 mg. *FFV* was calculated by the following equation:

$$FFV = 1 - \frac{1.3\rho V_w}{M}$$

where M is the molar mass (g mol^{-1}) of the repeat unit, V_w represents the van der Waals volume calculated by a literature method.[2]

Molecular dynamics (MD) simulations were used to calculate *FFV* according to a literature procedure[5] and measured de sities. An amorphous cell module in Materials Studio 8.0 was adopted for building simulation

models using ten polymer chains with a repeat unit of ten. Before running the procedure, 20 cycles of annealing were carried on at 300-1500 K. Then, cells were equilibrated by energy minimization, and several MD simulations were executed in a NPT ensemble (constant number of molecules, pressure = 1 atm, and temperature = 298.15 K) for more than 6 ns. After adjusting cell parameters, the cells reached the experimental densities. Afterwards, 20 cycles of annealing were performed at setting temperature ranging from 300 to 1500 K with NVT ensemble (constant number of molecules). Then, the cells were equilibrated by energy minimization and several MD simulations were performed in a NVT ensemble at the temperature of 298.15 K for more than 3 ns. The Atom Volumes and Surfaces module was adopted to measure the free volume and occupied volume with selection of 1.0 Å as the Connolly radius. Besides, pore size distributions (PSD) of CANAL-TBs were also simulated according to the reported method using Zeo++.[6] With the calculation by Monte Carlo sampling approach, the number of Monte Carlo samples per unit cell is set to 100,000 with a probe radius of 0.2 Å. The PSD scan range is 0-100 Å with 0.1 Å /step.

Gas permeation measurements were performed at 35 °C with a constant-volume/variable-pressure method. Gas permeability (*P*) was calculated according to the following equation:

$$P = D \times S = \frac{Vl}{ATp_{up} \times 0.278} \times \frac{dp}{dt} \times 10^{10}$$

where *P* (Barrer), *V* (cm^3), *l* (cm), *A* (cm^2), *T* (K), p_{up} (cmHg) and d*p*/d*t* represent pure gas permeation, downstream chamber volume, film thickness, effective membrane area, measurement temperature, upstream pressure, and increased rate of pressure in the downstream chamber at steady state, respectively. Diffusion coefficient (*D)* was estimated using lag time (ϑ) from the equation $D = l^2/6\vartheta$. Solubility coefficient (*S)* was calculated from the solution-diffusion mechanism ($S = P/D$).

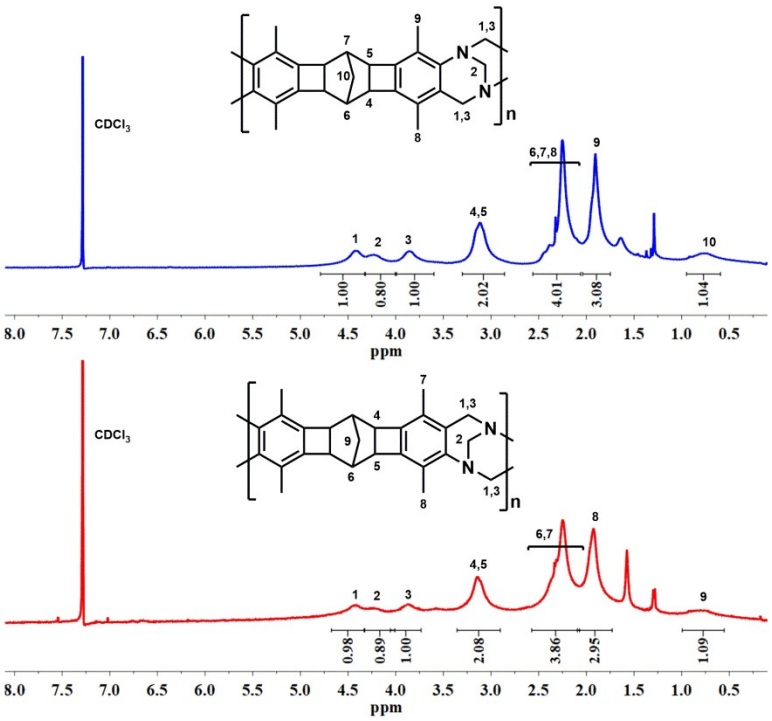

Figure S1. ^{1}H NMR spectra of *anti*-CANAL-TB-2 and *syn*-CANAL-TB-2.

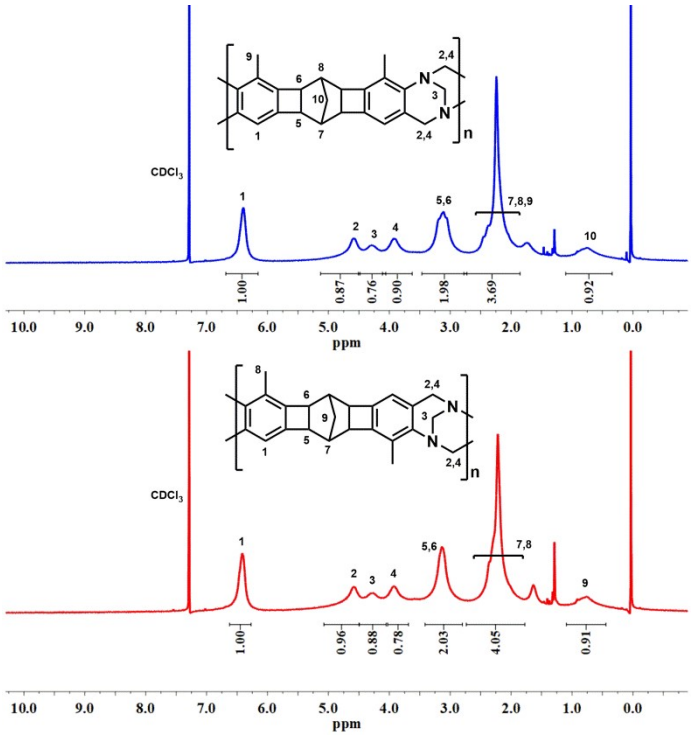

Figure S2. ^{1}H NMR spectra of *anti*-CANAL-TB-4 and *syn*-CANAL-TB-4.

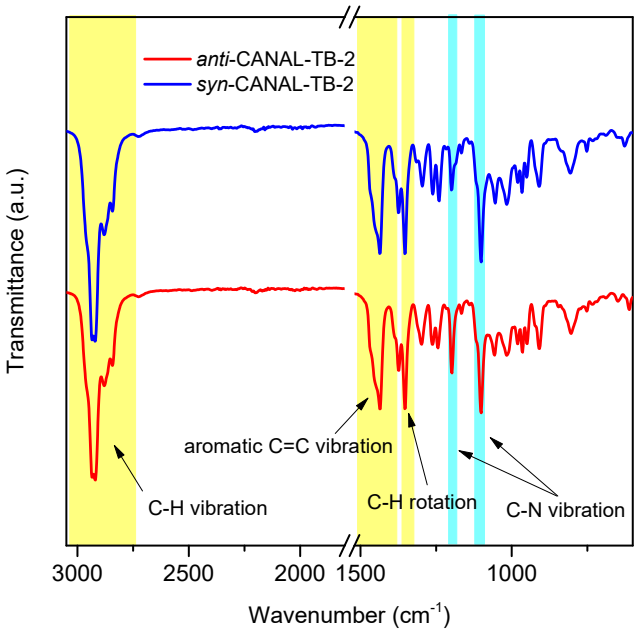

Figure S3. FT-IR spectra of *anti*-CANAL-TB-2 and *syn*-CANAL-TB-2.

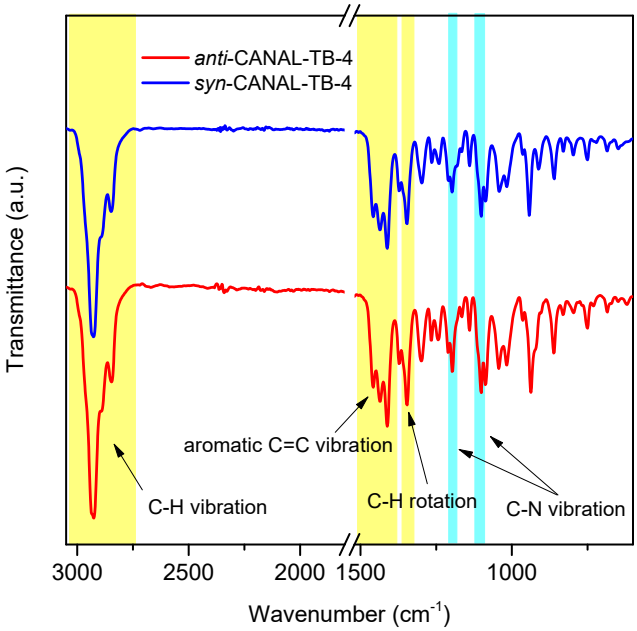

Figure S4. FT-IR spectra of *anti*-CANAL-TB-4 and *syn*-CANAL-TB-4.

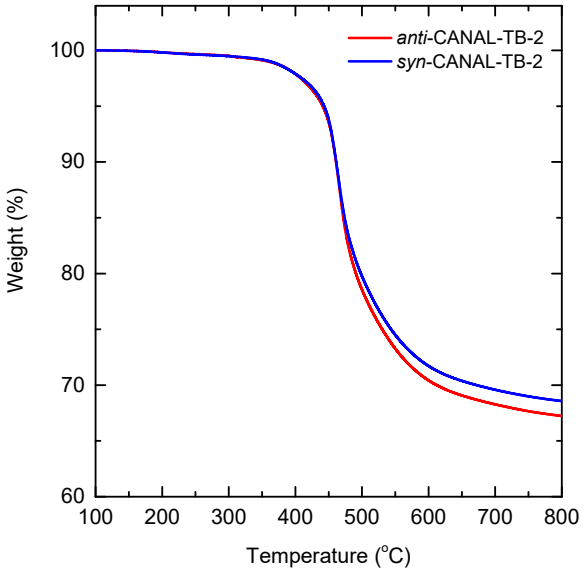

Figure S5. TGA curves of *anti*-CANAL-TB-2 and *syn*-CANAL-TB-2.

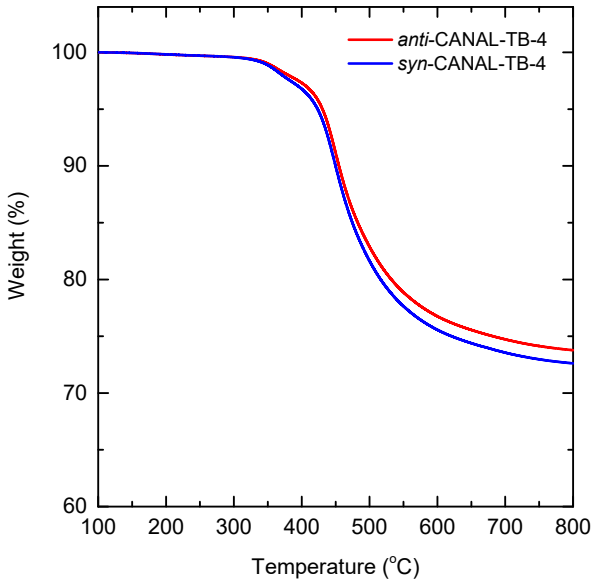

Figure S6. TGA curves of *anti*-CANAL-TB-4 and *syn*-CANAL-TB-4.

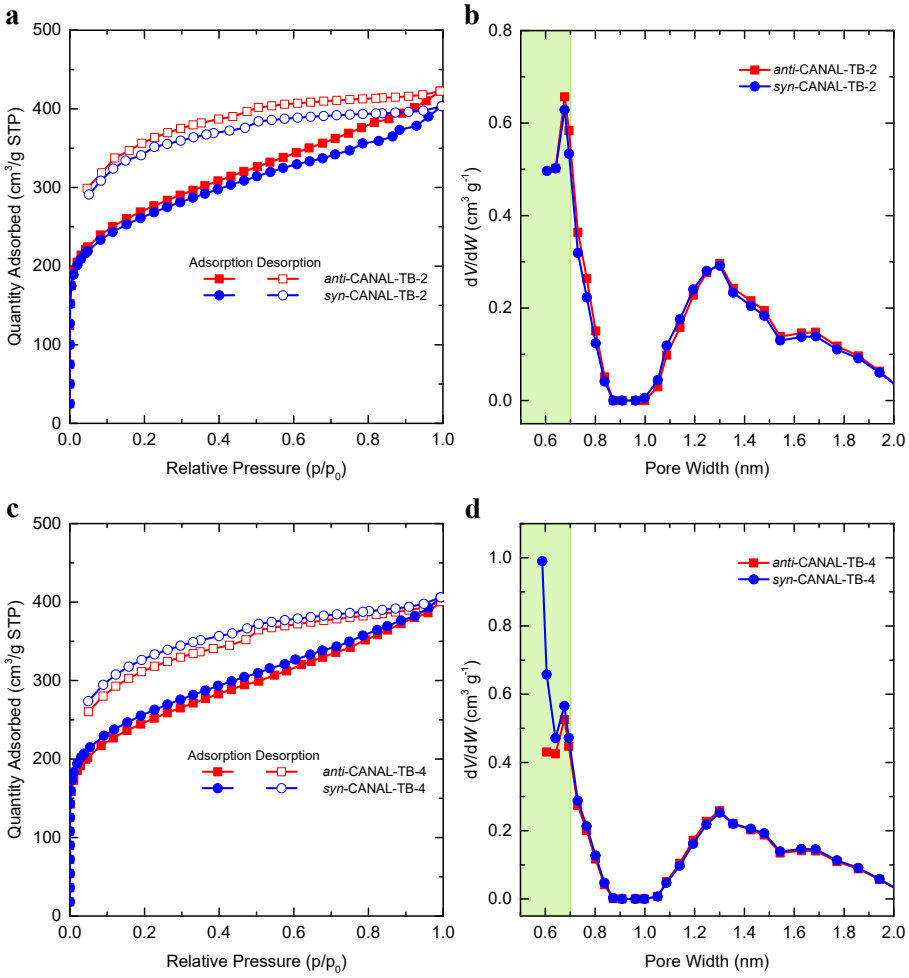

Figure S7. Microstructures of CANAL-TB polymers from pure regioisomers: **(a)** and **(c)** N_2 adsorption/desorption isotherms at 77 K; **(b)** and **(d)** pore size distributions calculated by N_2 sorption isotherms using NLDFT method.

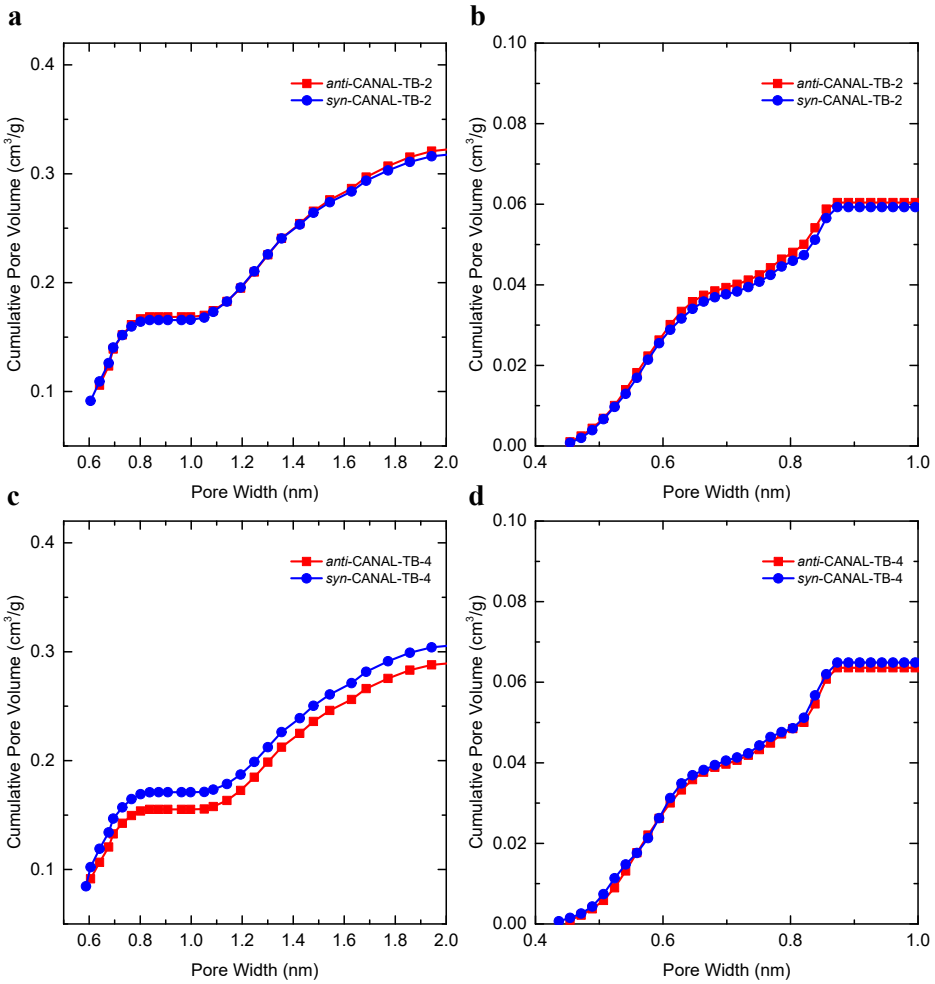

Figure S8. (a) Cumulative pore volumes of CANAL-TB-2 calculated from N_2 sorption isotherms; **(b)** cumulative pore volumes of CANAL-TB-2 calculated from CO_2 sorption isotherms; **(c)** cumulative pore volumes of CANAL-TB-4 calculated from N_2 sorption isotherms; **(d)** cumulative pore volumes of CANAL-TB-4 calculated from CO_2 sorption isotherms.

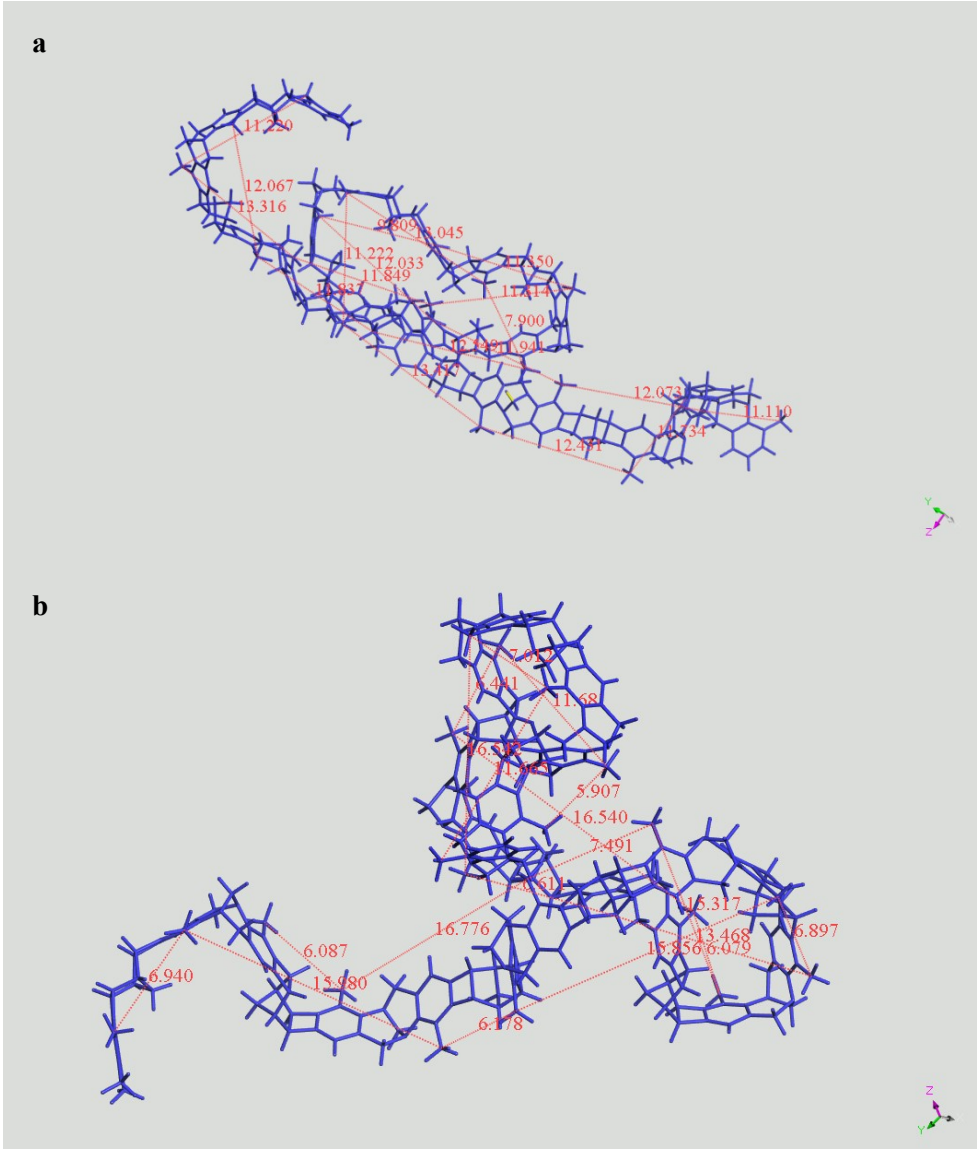

Figure S9. The distance of two *ortho*-methyl groups in a random chain of simulated model for *anti*-CANAL-TB-4 **(a)** and *syn*-CANAL-TB-4 **(b)**. (unit: Å)

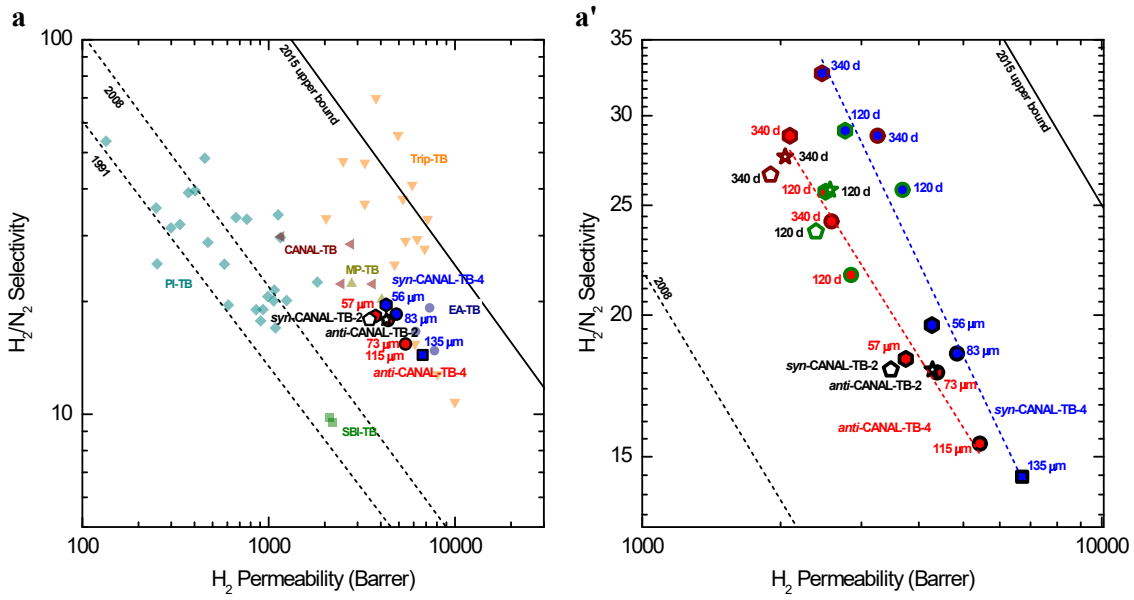

Figure S10. H_2/N_2 separation performance of *anti*-CANAL-TB-2 (open star symbols), *syn*-CANAL-TB-2 (open pentagons symbols), *anti*-CANAL-TB-4 (red solid symbols) and *syn*-CANAL-TB-4 (blue solid symbols), for comparison with previously published data of CANAL-TBs (wine solid left-triangles), PI-TBs (light cyan solid diamonds), SBI-TBs (light olive solid squares), EA-TBs (light navy solid circles), MP-TBs (light yellow solid up-triangles) and Trip-TBs (light orange solid down-triangles) (Table S1).

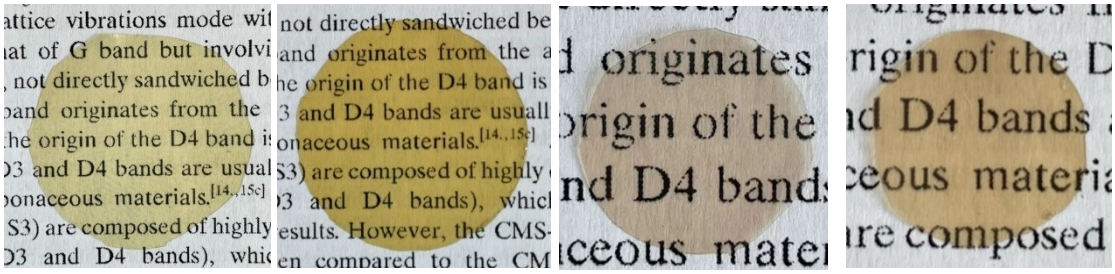

anti-CANAL-TB-4 *syn*-CANAL-TB-4 *anti*-CANAL-TB-2 *syn*-CANAL-TB-2

Figure S11. Photographs of CANAL-TB polymers from pure regio-isomers

Table S1. Gas permeabilities and selectivities of reported TB-based polymers

Polymers [Reference]	Permeability (Barrer)					Selectivity (α)			
	H_2	CO_2	O_2	N_2	CH_4	H_2/CH_4	H_2/N_2	O_2/N_2	CO_2/CH_4
CANAL-TB-1[2]	2760	1678	463	97	121	23	28	4.8	14
aged 300 days	1163	749	204	39	53	22	30	5.2	14
CANAL-TB-2[2]	3608	2520	747	162	205	18	22	4.6	12
aged 300 days	2452	1751	528	110	129	19	22	4.8	14
PI-TBs									
PI-TB-1[3]	607	457	119	31	27	22	20	3.8	17
PI-TB-2[3]	134	55	14	2.5	2.1	64	54	5.6	26
PI-TB-3[7]	299	218	42	10	6.7	45	31	4.4	33
PI-TB-4[7]	40	14	3.5	1.3	1.0	40	31	2.7	14
PI-TB-5[7]	54	20	4.9	1.9	1.7	32	28	2.6	12
CoPI-TB-1[8]	249	158	34	7.0	7.0	36	36	4.9	23
CoPI-TB-2[8]	403	209	53	10	10	40	40	5.2	21
CoPI-TB-3[8]	371	196	47	10	8.9	42	39	4.9	22
CoPI-TB-4[8]	667	241	96	20	18	37	34	4.8	13
CoPI-TB-5[8]	334	228	48	10	11	29	32	4.6	20
CoPI-TB-6[8]	472	330	73	16	19	25	29	4.5	17
Ac-CoPI-TB-1[9]	1826	1366	331	81	85	21	23	4.1	16
Ac-CoPI-TB-2[9]	1125	555	166	33	33	34	34	5.0	17
aged 348 days	454	205	49	9.4	8.3	55	48	5.2	25
Ac-CoPI-TB-3[9]	579	377	92	23	22	26	25	4.0	17
Ac-CoPI-TB-4[9]	252	203	38	10	10	25	25	3.8	20
PI-TB-N[9]	1156	731	185	39	38	30	30	4.7	19
aged 429 days	763	456	112	23	21	36	33	4.9	22
Bio-PITB-1-Vac[4]	906	1123	208	51	50	18	18	4.1	22
aged 100 days	856	1008	187	45	41	21	19	4.2	25
Bio-PITB-1-Air[4]	1088	1352	251	64	59	18	17	3.9	23
aged 100 days	933	1076	205	49	43	22	19	4.2	25
Bio-PITB-2-Vac[4]	1064	1201	237	53	49	22	20	4.5	25
aged 100 days	990	1087	214	48	40	25	21	4.5	27
Bio-PITB-2-Air[4]	1248	1384	267	62	59	21	20	4.3	23
aged 100 days	1073	1161	227	50	44	24	21	4.5	26
SBI-TBs									
PIM-SBI-TB (157 μm)[10]	2200	2900	720	232	450	5	9	3.1	6
PIM-SBI-TB (128 μm)[10]	2110	2720	657	215	406	5	10	3.1	7
EA-TBs									
PIM-EA-TB (181 μm)[10]	7760	7140	2150	525	699	11	15	4.1	10

aged 24 h	6155	4780	1590	370	502	12	17	4.3	10
PIM-EA-TB (95 μm)[10]	7310	5100	1630	380	572	13	19	4.3	9
MP-TBs									
PIM-MP-TB[11]	4050	3500	999	200	264	15	20	5.0	13
PIM-MP-TB (140 ^{o}C)[11]	2790	2340	648	125	158	18	22	5.2	15
Trip-TBs									
PIM-Trip-TB[12]	8039	9709	2718	629	905	9	13	4.3	11
aged 100 days	4740	3951	1073	189	218	22	25	5.7	18
PIM-BTrip-TB[13]	9980	13200	3290	926	1440	7	11	3.6	9
aged 166 days	4280	4150	1170	216	283	15	20	5.4	15
PIM-TMN-Trip-TB[14]	6100	6060	2030	396	710	9	15	5.1	9
CTTB (83 μm)[15]	7136	4676	1190	215	317	23	33	5.5	15
CTTB (54 μm)[15]	5257	3087	791	140	200	26	38	5.7	15
aged 150 days	2511	1228	334	53	72	35	47	6.3	17
CTTB (35 μm)[15]	3768	1402	374	54	67	56	70	6.9	21
MTTB (89 μm)[15]	6273	4441	1170	214	318	20	29	5.5	14
MTTB (60 μm)[15]	5897	3155	864	144	196	30	41	6.0	16
aged 150 days	3283	1693	440	70	92	36	47	6.3	18
MTTB (37 μm)[15]	4950	2257	580	89	118	42	56	6.5	19
ITTB (87 μm)[15]	6880	4992	1318	249	374	18	28	5.3	13
ITTB (54 μm)[15]	5423	3901	1012	187	276	20	29	5.4	14
aged 150 days	2034	1370	354	61	83	25	33	5.8	17
ITTB (35 μm)[15]	3280	2063	508	90	115	29	36	5.6	18

Table S2. Diffusion/solubility coefficients and selectivities of CANAL-TB polymers

Polymer	*D* (10^{-8} cm^2/s)				*S* (10^{-2} cm^3/cm^3 $cmHg^{-1}$)				O_2/N_2		CO_2/CH_4	
	O_2	N_2	CH_4	CO_2	O_2	N_2	CH_4	CO_2	α_D	α_S	α_D	α_S
anti-CANAL-TB-4 (115 μm)	214 ±16	63.0 ±8	24.4 ±1	70.6 ±11	6.39 ±0.8	5.60 ±0.7	14.9 ±2	44.2 ±2	3.39	1.14	2.90	2.95
anti-CANAL-TB-4 (57 μm)	127 ±9	34.2 ±2	12.6 ±3	39.1 ±3	6.94 ±1	5.99 ±0.4	16.6 ±0.8	57.0 ±5	3.72	1.16	3.10	3.43
syn-CANAL-TB-4 (135 μm)	244 ±11	71.7 ±6	30.2 ±2	90.0 ±5	7.22 ±0.6	6.48 ±0.9	15.1 ±1	39.6 ±3	3.41	1.11	2.96	2.63
syn-CANAL-TB-4 (56 μm)	191 ±13	43.8 ±11	15.6 ±7	50.3 ±8	5.03 ±0.4	4.98 ±0.5	14.3 ±0.6	47.7 ±0.9	4.36	1.01	3.22	3.34
anti-CANAL-TB-2 (59 μm)	204 ±24	57.7 ±5	18.5 ±2	54.6 ±4	4.90 ±0.7	4.14 ±0.2	13.9 ±1	45.2 ±2	3.54	1.18	2.95	3.25
syn-CANAL-TB-2 (61 μm)	182 ±18	48.9 ±8	16.6 ±5	48.3 ±6	4.31 ±1	3.97 ±0.2	13.5 ±0.7	43.7 ±0.8	3.72	1.09	2.91	3.24
CANAL-TB-1[2]	94	22.2	7.01	34.7	4.92	4.37	17.3	48.3	4.22	1.13	4.95	2.80
CANAL-TB-2[2]	175	44	11.4	58.0	4.27	3.68	18.0	43.4	3.98	1.16	5.09	2.42
Bio-PITB-1[4]	135	22.7	4.58	18.4	1.85	2.82	13.0	73.6	5.96	0.66	4.01	5.67
Bio-PITB-2[4]	60.4	12.8	3.45	16.4	4.43	4.82	17.3	84.8	4.71	0.92	4.73	4.90
PIM-SBI-TB[10]	201	75.2	31.5	74	3.58	3.09	14.3	39.2	2.67	1.16	2.35	2.74
PIM-EA-TB[10]	318	99.5	36	87	6.76	5.28	19.4	82.1	3.20	1.28	2.42	4.23
PIM-MP-TB[11]	106	18.3	6	26	9.42	10.9	44	135	5.79	0.86	4.33	3.07
PIM-Trip-TB[12]	462	135	48.9	111	5.88	4.66	18.5	87.5	3.42	1.26	2.27	4.73
PIM-BTrip-TB[13]	347	70	28	99	9.48	13.2	51.4	133	4.95	0.72	3.53	2.59

Table S3. Gas permeability and ideal selectivity of the aged CANAL-TB polymers

Polymer	Permeability (Barrer)					Selectivity			
	H_2	CO_2	O_2	N_2	CH_4	H_2/CH_4	H_2/N_2	O_2/N_2	CO_2/CH_4
anti-CANAL-TB-2 (59 μm)									
aged 120 days	2564±69	1368±37	470±15	99±3	110±9	23.3	25.8	4.75	12.43
aged 340 days	2048±62	1048±29	358±9	74±1	84±2	24.4	27.6	4.84	12.50
syn-CANAL-TB-2 (61 μm)									
aged 120 days	2389±74	1285±40	445±13	101±7	123±6	19.4	23.7	4.41	10.46
aged 340 days	1902±48	1028±21	328±17	72±2	91±1	20.9	26.6	4.56	11.29
anti-CANAL-TB-4 (73 μm)									
aged 120 days	2849±57	1442±33	609±20	131±6	139±4	20.5	21.7	4.64	10.38
aged 340 days	2581±49	1249±38	505±18	107±7	118±4	21.9	24.2	4.73	10.58
anti-CANAL-TB-4 (57 μm)									
aged 120 days	2506±53	1271±25	463±11	97±2	116±7	21.6	25.7	4.75	10.96
aged 340 days	2096±63	972±32	354±14	73±4	79±1	24.1	28.8	4.87	11.17
syn-CANAL-TB-4 (83 μm)									
aged 120 days	3687±85	1728±39	692±26	143±6	160±8	23.0	25.8	4.84	10.79
aged 340 days	3253±79	1510±56	570±19	113±8	134±5	24.3	28.8	5.04	11.26
syn-CANAL-TB-4 (56 μm)									
aged 120 days	2765±55	1324±42	486±12	95±5	95±2	29.0	29.1	5.11	13.87
aged 340 days	2462±68	1069±28	395±15	75±2	77±3	32.0	32.7	5.24	13.88

References

(1) Abdulhamid, M. A.; Lai, H. W. H.; Wang, Y.; Jin, Z.; Teo, Y. C.; Ma, X.; Pinnau, I.; Xia, Y., Microporous Polyimides from Ladder Diamines Synthesized by Facile Catalytic Arene–Norbornene Annulation as High-Performance Membranes for Gas Separation. *Chem. Mater.* **2019,** *31* (5), 1767-1774.

(2) Ma, X.; Lai, H. W. H.; Wang, Y.; Alhazmi, A.; Xia, Y.; Pinnau, I., Facile Synthesis and Study of Microporous Catalytic Arene-Norbornene Annulation–Tröger's Base Ladder Polymers for Membrane Air Separation. *ACS Macro Lett.* **2020,** *9*, 680-685.

(3) Zhuang, Y.; Seong, J. G.; Do, Y. S.; Jo, H. J.; Cui, Z.; Lee, J.; Lee, Y. M.; Guiver, M. D., Intrinsically Microporous Soluble Polyimides Incorporating Tröger's Base for Membrane Gas Separation. *Macromolecules* **2014,** *47* (10), 3254-3262.

(4) Hu, X.; Lee, W. H.; Bae, J. Y.; Zhao, J.; Kim, J. S.; Wang, Z.; Yan, J.; Lee, Y. M., Highly permeable polyimides incorporating Tröger's base (TB) units for gas separation membranes. *J. Membr. Sci.* **2020,** *615*, 118533.

(5) Zhang, C.; Li, P., Preparation and Gas Separation Properties of Spirobichroman-Based Polyimides. *Macromol. Chem. Phy.* **2018,** *219* (16), 1800157.

(6) Willems, T. F.; Rycroft, C. H.; Kazi, M.; Meza, J. C.; Haranczyk, M., Algorithms and tools for high-throughput geometry-based analysis of crystalline porous materials. *Microporous Mesoporous Mater.* **2012,** *149* (1), 134-141.

(7) Zhuang, Y.; Seong, J. G.; Do, Y. S.; Lee, W. H.; Lee, M. J.; Guiver, M. D.; Lee, Y. M., High-strength, soluble polyimide membranes incorporating Tröger's Base for gas separation. *J. Membr. Sci.* **2016,** *504*, 55-65.

(8) Zhuang, Y.; Seong, J. G.; Do, Y. S.; Lee, W. H.; Lee, M. J.; Cui, Z.; Lozano, A. E.; Guiver, M. D.; Lee, Y. M., Soluble, microporous, Tröger's Base copolyimides with tunable membrane performance for gas separation. *Chem. Commun.* **2016,** *52* (19), 3817-3820.

(9) Zhang, Y.; Lee, W. H.; Seong, J. G.; Bae, J. Y.; Zhuang, Y.; Feng, S.; Wan, Y.; Lee, Y. M., Alicyclic segments upgrade hydrogen separation performance of intrinsically microporous polyimide membranes. *J. Membr. Sci.* **2020,** *611*, 118363.

(10) Carta, M.; Malpass-Evans, R.; Croad, M.; Rogan, Y.; Jansen, J. C.; Bernardo, P.; Bazzarelli, F.; McKeown, N. B., An efficient polymer molecular sieve for membrane gas separations. *Science* **2013,** *339* (6117), 303-307.

(11) Williams, R.; Burt, L. A.; Esposito, E.; Jansen, J. C.; Tocci, E.; Rizzuto, C.; Lanč, M.; Carta, M.; McKeown, N. B., A highly rigid and gas selective methanopentacene-based polymer of intrinsic microporosity derived from Tröger's base polymerization. *J. Mater. Chem. A* **2018,** *6* (14), 5661-5667.

(12) Carta, M.; Croad, M.; Malpass-Evans, R.; Jansen, J. C.; Bernardo, P.; Clarizia, G.; Friess, K.; Lanč, M.; McKeown, N. B., Triptycene Induced Enhancement of Membrane Gas Selectivity for Microporous Tröger's Base Polymers. *Adv. Mater.* **2014,** *26* (21), 3526-3531.

(13) Rose, I.; Carta, M.; Malpass-Evans, R.; Ferrari, M.-C.; Bernardo, P.; Clarizia, G.; Jansen, J. C.; McKeown, N. B., Highly Permeable Benzotriptycene-Based Polymer of Intrinsic Microporosity. *ACS Macro Lett.* **2015,** *4* (9), 912-915.

(14) Rose, I.; Bezzu, C. G.; Carta, M.; Comesaña-Gándara, B.; Lasseuguette, E.; Ferrari, M. C.; Bernardo, P.; Clarizia, G.; Fuoco, A.; Jansen, J. C.; Hart, Kyle E.; Liyana-Arachchi, T. P.; Colina, C. M.; McKeown, N. B., Polymer ultrapermeability from the inefficient packing of 2D chains. *Nat. Mater.* **2017,** *16* (9), 932-937.

(15) Zhu, Z.; Zhu, J.; Li, J.; Ma, X., Enhanced Gas Separation Properties of Tröger's Base Polymer Membranes Derived from Pure Triptycene Diamine Regioisomers. *Macromolecules* **2020,** *53* (5), 1573-1584.